

Determination of Tensile Properties of Polyester – Industrial Waste Red Mud Composites Using Digital Image Correlation (DIC)

Marcelo Rodrigues^{a*} , Maurício Maia Ribeiro^b , Robson Luis Baleeiro Cardoso^c ,
Ana Gabriele da Paixão Ferreira^a , Silmara Mota Cardoso^a , Jaciléa Campos da Silva^a ,
Roberto Paulo Barbosa Ramos^a , Jean da Silva Rodrigues^a 

^aInstituto Federal de Educação, Ciência e Tecnologia do Pará, Programa de Engenharia de Materiais, 66093-020, Belém, PA, Brasil.

^bInstituto Federal de Educação, Ciência e Tecnologia do Pará, 67125-000, Ananindeua, PA, Brasil.

^cUniversidade Federal do Pará, Programa de Engenharia de Recursos Naturais da Amazônia, 66075-110, Belém, PA, Brasil.

Received: October 17, 2022; Revised: February 23, 2023; Accepted: March 30, 2023

The Digital Image Correlation (DIC) technique is an important method of evaluating material strain fields. Composite materials have inherently heterogeneous elastic properties, in the function of the different phases present in the composition, whereat the traditional techniques of deformation evaluation may not be sufficient to determine the mechanisms that eventually contribute to the failure of the material. The present work were evaluated, the tensile mechanical properties of polyester matrix composites loaded with an industrial residue of red mud, with a mass fraction of 20%. The properties were surveyed using the conventional technique of strain gauge and compared with the data obtained through DIC. The results showed that the DIC technique was accurate in monitoring the displacements and determining the average deformation of the tested specimens, in addition to providing ample deformation fields, for the evaluation of failure mechanisms throughout the sample request process.

Keywords: Red mud, tensile properties, DIC, polyester composites.

1. Introduction

The Digital Image Correlation (DIC) technique is one of the main methods for measuring deformations of materials with applications in industry, in biomechanics, in experimental mechanics, among other areas¹.

Through DIC it is possible to obtain the full-field displacements and strains by means of the use of correspondence procedures based on correlation and numerical differentiation algorithms. The data are obtained by comparing several images captured during the mechanical test².

Composites represent a challenge to the characterization processes either by their intrinsically heterogeneous nature or by the presence of defects, such as porosity, fiber misalignment, particle agglomeration, or even holes and notches, which can nucleate or potentiate the propagation of cracks, being vital the accurate tracking of the deformations when it occurs a material solicitation.

In this sense, the conventional technique to determinate the deformation only provides the average deformation of the area under clip, using electric extensometer, or punctual strains restricted to the contact area, in the case of strain gauges. DIC, in turn, can both provide equivalent measures to conventional techniques and allow the visualization of the full-field deformation of the entire surface of the sample

under test, allowing the precise study of the mechanisms that eventually lead the part to fail.

The main objective of using the DIC technique is to monitor the progress of damage in specimens subjected to load application, based on the recognition of a speckles pattern created on the surface to be analyzed, and its difference before and after load application³, allowing, by identifying the failure mechanisms, to develop a design model suitable for the observations⁴ make accurate DIC measurements, a good speckles pattern must meet several requirements, such as high contrast, randomness, isotropy, and stability. Different speckles patterns can be realized by different operators using the same techniques because technology and parameters play a key role in each technique⁵.

The DIC technique is operationalized through the capture of subsequent images, usually by means of CCD cameras, of a sample under mechanical request, on which the speckle is applied. After applying the speckle, the sample image is then registered before deformation, called reference image. A virtual grid is applied over this, establishing points of interest that will be tracked in the subsequent registered image, after the deformation, referred to as deformed image.

The pixel that contains the point of interest and its neighbors thus compose a unique subset¹ on the reference image and can be correlated with the same subset to be tracked in the deformed image. The longitudinal and transverse

*e-mail: marcelo.rodrigues@ifpa.edu.br

displacements recorded from the subset between the two images thus compose the full-field displacement, which are finally differentiated to generate the deformation fields.

DIC can be applied both for the evaluation of deformation occurring in the plane when it is called DIC-2D, that three-dimensional deformations which require two or more capture cameras working simultaneously (DIC-3D).

Several researchers have sought to develop particulate composites using industrial residues from red mud, in the function of the high volume of this material generated annually and the risks to the environment inherent to its accumulation process.

Red mud is a by-product of the caustic leaching of bauxite during industrial alumina production. About 1 to 2 tons of red mud residue is produced for every ton of alumina, most being stored or thrown overboard with very little reuse⁶.

Red mud is disposed of in landfills and stored for a long period in large lagoon-type dams. It is a threat to the environment and is not economically sustainable due to increasing consolidation. This leads to an urgent need to develop new improved techniques for the proper storage and disposal of these wastes. New materials can be developed to effectively manage red mud, such as composites, which can reduce or prevent its storage⁷.

In addition to the environmental gain, the use of red mud in composites can contribute to its stiffening and increase the tensile and compressive strength of the samples. Red mud has been used as a reinforcement in polyester and epoxy matrix composites⁷, as one of the phases of polyester/sisal fiber/red mud hybrids⁸ or polyester/fiber coconut/red mud⁹, replacing fly ash in the production of cement composites¹⁰, among others.

The addition of red mud to polymer matrices subjected to tensile stress contributes to an increase in the modulus of elasticity¹¹ and the tensile resistance limit¹², however, for the latter, the gain is perceived up to a limit of 20% mud mass fraction^{6,7,13} on average, from which the red mud is unable to disperse properly due to its high surface energy and agglomerates leading to an inhomogeneous dispersion in the matrix, reducing the resistance¹⁴. Then, the boundary of the 20% red mud inclusion is an important point for the verification of the full-field deformation.

In this work, the DIC-2D technique was applied to composites reinforced with industrial residue of red mud, with a mass fraction of 20%. Longitudinal deformations were measured using an electric clip-on-extensometer. The full-field strain and the average strains in the longitudinal and transverse directions of the sample under test were determined using the DIC technique. The results of the two techniques were statistically compared to assess the technique's precision.

2. Material and Methods

2.1. Materials

The matrix used was terephthalic unsaturated polyester resin (Arazyn AZ 1.0 #34) of medium viscosity with a healing agent of the type methyl ethyl ketone peroxide (MEK_p), both supplied by Ara Química SA (São Paulo, Brazil), added at 1 wt% in relation to the resin mass. The red mud, industrial residue from the Bayer process for obtaining alumina, was provided by Hydro Alunorte in Barcarena, Pará, Brazil.

2.2. Red mud characterization

The red mud residues were dried in a recirculation oven for approximately 24 (twenty-four) hours at 105°C. Then, the procedure applied to adjust its granulometry was done manually in a 100-mesh sieve of the Tyler series, the passing material, shown in Figure 1, which was used to make the composites.

To identify the chemical composition of the residues, an X-ray Fluorescence equipment was used, Bruker, model S2 – Ranger, with samples as pressed pellets.

Morphological and microstructural analyzes were performed using a Scanning Electron Microscope (SEM), model VEGA 3 SBU from TESCAN. The determination of the specific mass of the red mud residue followed the psychometric method using distilled water and 3 samples of approximately 1.0g of particulates.

2.3. Composites preparation

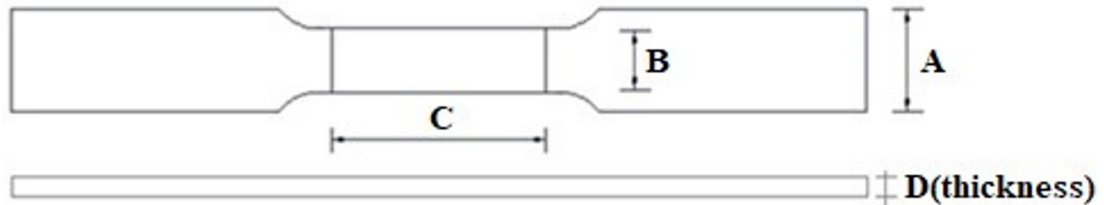
The composites were fabricated with a mass fraction of red mud in the polyester matrix of 20%, following the geometry established in the ASTM D638 standard. The red



Figure 1. (a) Red mud residue before comminution and (b) after hand sieving through a 100 mesh.

Table 1. Dimensions (mm).

Specimens	A	B	C	D
CP01LV20	19.2	9.80	70	2.97
CP02LV20	19.4	9.77	70	3.10
CP03LV20	19.4	9.80	70	3.90
CP04LV20	19.3	9.70	70	2.97
CP05LV20	19.2	9.73	70	3.43
CP06LV20	19.6	10.03	70	2.97


Figure 2. Test specimen dimension references.

mud was initially dried, then added to the polyester matrix and homogenized with a mechanical mixer. After adding MEK-p, the mixture was then poured into silicone molds and cured at room temperature.

Six samples were manufactured for the tensile test, which are named sequentially in Table 1, with dimensions according to Figure 2.

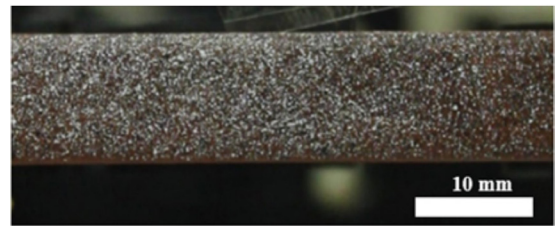
2.4. Tensile test

The fabricated specimens were initially speckled on one side, for the application of the DIC technique, using white and black spray paint (Figure 3). On the opposite side of the samples, it was affixed an electrical Clip-on Extensometer type SANJ blade, Model YSJ90/10-ZC (Figure 4a) to determine the longitudinal strains. The extensometer was interfaced with a computer (Figure 4c) through a 6-channel Didaq B2 module (Figure 4b).

2.5. Digital image correlation (DIC)

The tensile tests were performed according to the procedures of ASTM D638¹⁵, with a test speed of 2 mm/min, using a universal testing machine AROTEC WDW 100E (IFPa, Belém, Pará, Brazil), with a load cell of 5 kN. For application the DIC technique, digital images were obtained using a CANON digital camera, model EOS REBEL T3i, EF-S 18-55mm lens, 18-megapixel resolution. Illumination was done through an LED lamp, 7W, 600 lumens, 6.500K. The camera's focus is concentrated on the surface of the object to record successive images of the speckle pattern under load application¹⁶. The modulus of elasticity was determined by the ratio between the difference between two stress points and the difference between their corresponding strain pairs, as established in ASTM D638¹⁵.

For the application of DIC was used the Omnivid-DIC 2D software, developed at PPGEMAT/IFPA (Belém, Pará, Brazil), applying a rectangular grid (30 lines x 5 columns)


Figure 3. Speckle pattern applied on polyester/red mud specimens.

on the speckle, as illustrated in Figure 5. The deformations in the longitudinal and transverse directions were calculated by averaging the deformation of the grid on each axis. From each test, 200 images were generated which were subsequently evaluated to determine deformations.

2.6. Statistical analysis

Analysis of variance (ANOVA) was used, through the F test, to verify if there were significant differences between the means of the deformation results and elastic modulus obtained in the mechanical test through the extensometer and DIC. To compare the means of treatment, Tukey's Significant Difference test was applied (posttest), if necessary. The significance level adopted was (α) of 5%, with the null hypothesis (H_0) being equivalence between means; in which for P-value smaller than α , reject if H_0 . Statistical analysis was conducted entirely using the R CORE TEAM Environment (2020), using the RSTUDIO TEAM (2020) integrated development environment, and supported by additional packages.

The value of the minimum significant difference (m.s.d.) was found through Equation 1:

$$m.s.d. = q \cdot \sqrt{\frac{QMR}{n}} \quad (1)$$

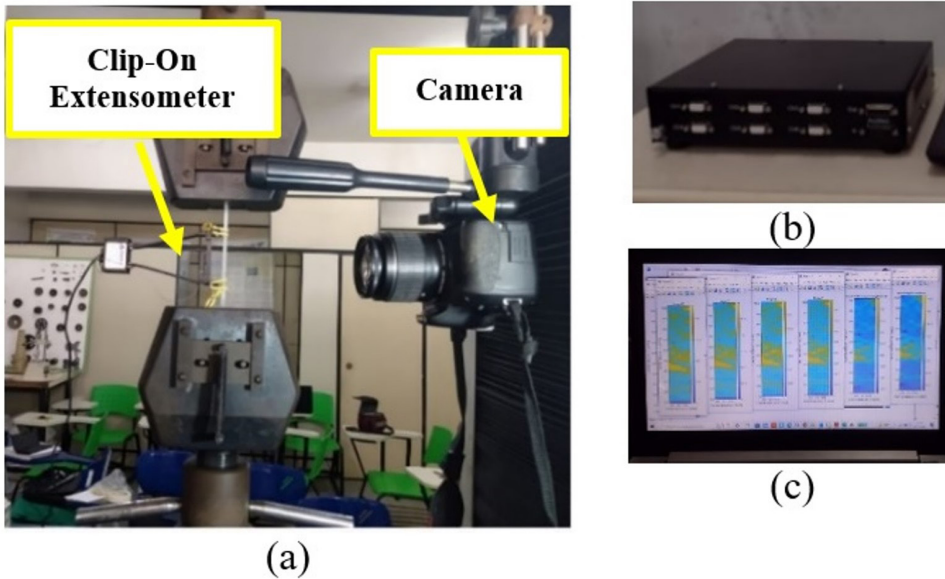


Figure 4. (a) Experimental setup with extensometer for mechanical testing of composites (tensile test); (b) Didaq B2 module and (c) Computer.

Where:

q = Total student amplitude (tabulated value), which is a function of the degree of freedom of the residue (GLR) and number of treatments.

QMR = Mean square of residue within the group;

n = Number of repetitions of each treatment within the group;

3. Results and Discussion

3.1. Characterization of red mud waste

The specific mass result obtained for the red mud was 2.04 ± 0.06 g/cm³. This specific mass value of the red mud residue is similar to those found by Liu and Poon¹⁷ and Wang et al.¹⁸, which resulted, respectively, in 2.18 g/cm³ and 2.21 g/cm³.

The granulometry of red mud was defined as material passing through the 100 mesh sieve of the Tyler series, which allows residue to pass below 0.149mm.

3.2. Scanning electron microscopy

Figure 6 shows the image of the red mud residue sample obtained from the scanning electron microscopy (SEM).

It is observed that there is a heterogeneous and irregular granulometric distribution, with the presence of fine particles that tend to agglomerate¹⁹. These agglomerated particulates tend to form relatively larger aggregates^{20,21}.

3.3. X-Ray fluorescence

Table 2 indicates the nominal composition (amount % mass) of the oxide contents of the red mud residue obtained by X-Ray Fluorescence (XRF) analysis. It is observed that the red mud residue is mainly composed of several oxides, the most abundant chemical component is Fe₂O₃ (Hematite) with 33.70%, followed by Al₂O₃ (Alumina) with 22.90%,

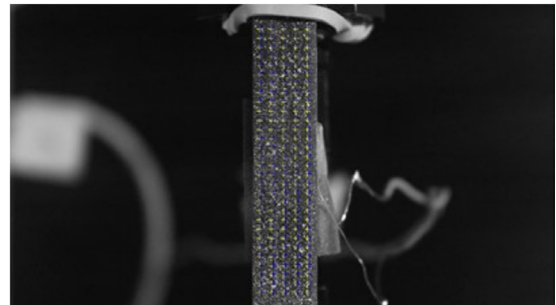


Figure 5. Rectangular grid 30x5 applied on the speckle to determine the longitudinal and transverse deformation.

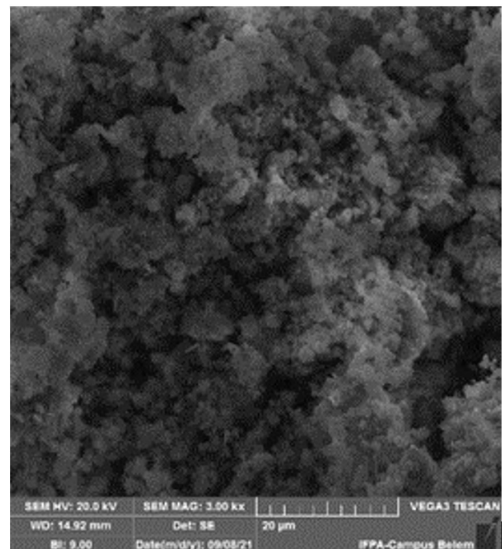


Figure 6. Red mud residue sample, 3kx.

SiO₂ (Silica) with 19.40% and Na₂O (Oxide of sodium) with 13.50%. The chemical properties and utilization of red mud mainly depend on these four components. In addition, TiO₂ (Titanium Dioxide) with 5.67% and CaO (Calcium Oxide) with 1.09% represent a small proportion, and other components represent a minor proportion, and these components have almost no effect on the red mud. Several researchers also performed X-Ray Fluorescence (FRX) analysis of the red mud residue in their research, as shown in Table 3.

3.4. Tensile mechanical properties of Composites

Table 4 illustrates the results obtained in the tensile test of polyester/red mud composites, calculated using the strain gauge and by DIC. The samples showed a tensile strength limit of 14.973 MPa, very close to the value obtained by Prabu et al.⁷ which resulted in 14.30 MPa, working with polyester and 20 wt% red mud.

The average value obtained for the modulus of elasticity was 0.6621 GPa and for the failure strain 0.0393 mm/mm, calculated from the results of the strain gauge. By means of DIC, it was obtained for the modulus, 0.6766 GPa and for the strain 0.0387 mm/mm, presenting errors in the DIC versus Extensometer ratio, of +2.20% and -1.61%, respectively. Figure 7 illustrates the stress-strain diagram obtained by using each technique for the six specimens tested.

Quanjin et al.²⁵ testing pure epoxy polymer under traction, obtained the deformations by means of DIC and compared with those acquired using strain gauges, finding, for the modulus of elasticity, average differences of 9.60%.

The analysis of Figure 7 proves the accuracy of the deformation measurements obtained via the digital image correlation method, concerning the conventional technique used.

Significant differences are only observed in samples 2 and 6. Figure 8 illustrates the maximum, mean and minimum

differences verified between the deformations obtained via strain gauge and via DIC for the samples tested, where it is verified that, except for samples 2 and 6, the others showed a mean difference of less than 0.1%.

The maximum difference observed in sample 2 (CP02LV20) was in the order of 0.3844% (0.003844 mm/mm) and in sample 6 in 0.193%. Castillo et al.⁴ obtained differences of up to 0.06% in samples of epoxy matrix composite with fibrous reinforcement, with longitudinal strains determined via DIC compared to those obtained via strain gauges.

3.5. Full-field deformation

Figure 9 illustrates the graphs of mean strain in the longitudinal and transverse directions, in addition to the final full-field deformation in each direction. In (Figure 9a), it is possible to verify the evolution of deformations as a function of the analyzed image, evidencing the deformation jump that indicates the rupture of the sample. The images generated after the fracture were not considered for the analysis, as well as the deformation jump, for the comparison of the deformations obtained in each measurement technique.

The transverse strain fields (Figure 9b) do not indicate strain concentration in the region of interest, not even in the vicinity of the fracture zone, which corroborates the results normally found for polymeric composites with particulate reinforcement, of low transverse strain and without expressive section reduction in the fracture region, typical of materials with tendencies to fragile fracture. In Figure 9c, one can see the high strain levels concentrated in the fracture area.

Figure 10 illustrates the partial longitudinal strain fields that were recorded in the sample request CP02LV20. The deformations, initially well distributed, present a slight concentration around the 600-pixel elevation in the longitudinal direction, however, the fracture occurs abruptly, in the region of the 280-pixel elevation of the area of interest.

Table 2. Nominal composition (amount % mass), in oxides, of Red Mud.

Residue	Na ₂ O	MgO	Al ₂ O ₃	SiO ₂	SO ₃	Cl	K ₂ O	CaO	TiO ₂	Fe ₂ O ₃	ZrO ₂
Red Mud Residue	13.50	0.896	22.90	19.40	0.378	0.447	0.330	1.09	5.67	33.70	0.822

Table 3. Main nominal compositions (amount % mass), in oxides, red mud residue presented in the literature.

Residue	Fe ₂ O ₃	Al ₂ O ₃	SiO ₂	Na ₂ O	TiO ₂	References
Red Mud Residue	37.00	22.80	14.10	11.50	7.92	Yoon et al. ²²
	38.82	21.66	20.26	11.38	4.58	Qiu et al. ²³
	34.30	21.40	20.10	8.10	2.00	Ma et al. ²⁴

Table 4. Result of tensile tests of samples of red mud polyester composites.

Material Composite	Tensile Strength (MPa)	Modulus of Elasticity E (GPa)			Failure Strain (mm/mm)		
		by Extensometer	by DIC	Error (%) DIC vs Ext.	by Extensometer	by DIC	Error (%) DIC vs Ext.
Polyester/ 20wt% Red Mud	14.973	0.6621±0.0508	0.6766±0.0664	+ 2.20	0.0393±0.0077	0.0387±0.0084	- 1.61

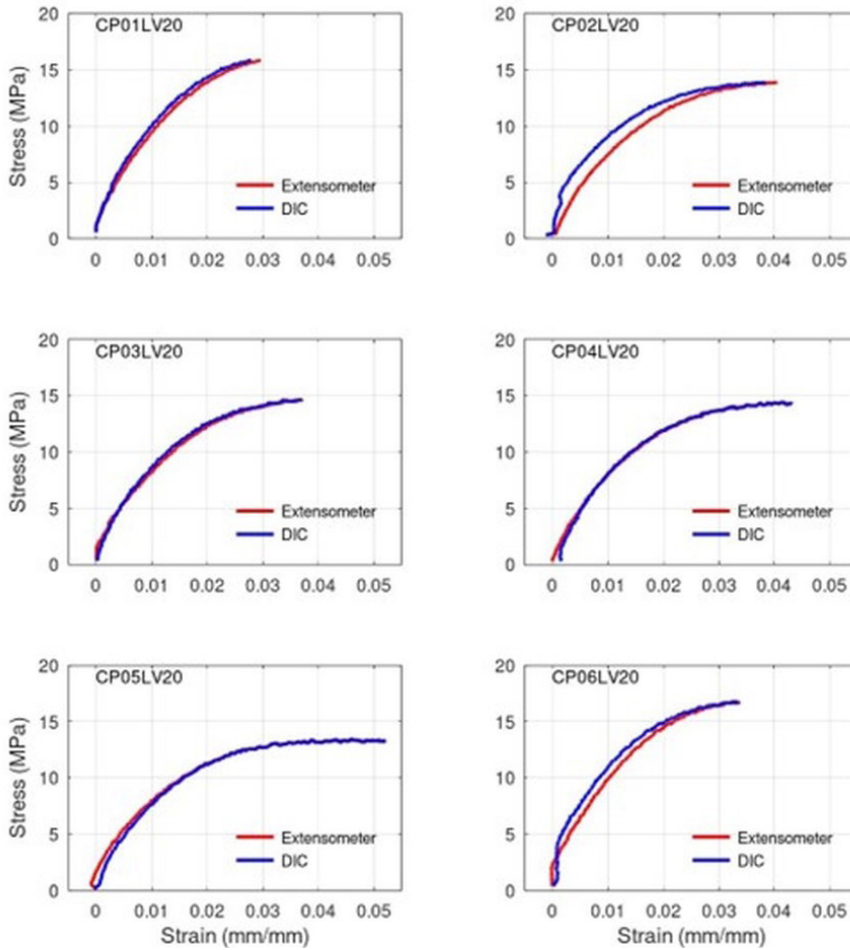


Figure 7. Stress x strain diagram of polyester matrix composites with 20wt% red mud with strains obtained via electrical strain gauge and via DIC.

It can then be inferred that, despite the high mass fraction of red mud particles in the polymer matrix, with a high tendency to agglomerate, the failure mechanism cannot be identified, and the fracture region was not previously located, probably due to the intrinsic characteristic of the sudden fracture samples and the displacement rates used during the test, 2 mm/min. In addition, the technique used, DIC-2D, can only demonstrate the superficial effects caused by the internal defects of the sample, which will not necessarily be revealed on the face under observation.

The incorporation of red mud restricts the molecular mobility of the polymeric chains in the composite and reduces the ductility of the matrix¹³, enhancing the tendency to sudden fracture presented by particulate polymeric composites.

Figure 11 illustrates the cross-section of one of the samples where the formation of several points of agglomeration of red mud is verified, due to the high load of mud inserted in the matrix (20wt%).

The fracture surface shown in Figure 11 illustrates the formation of several agglomerates of particulate matter, which, as also observed by Liu et al.¹³ can lead to stress concentration, decreasing the tensile strength of the composite.

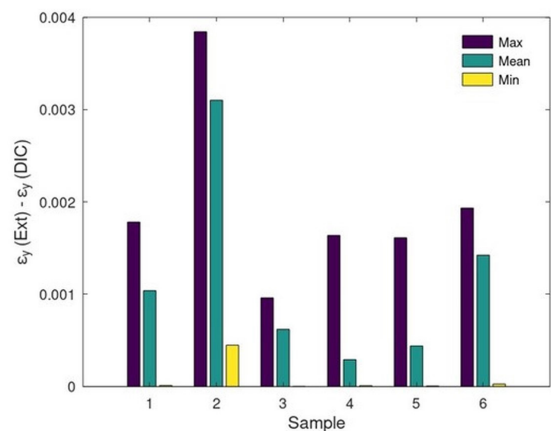


Figure 8. Maximum, mean and minimum differences.

3.6. Statistical analysis

Statistical analyzes of longitudinal strain and modulus of elasticity are presented in Table 5.

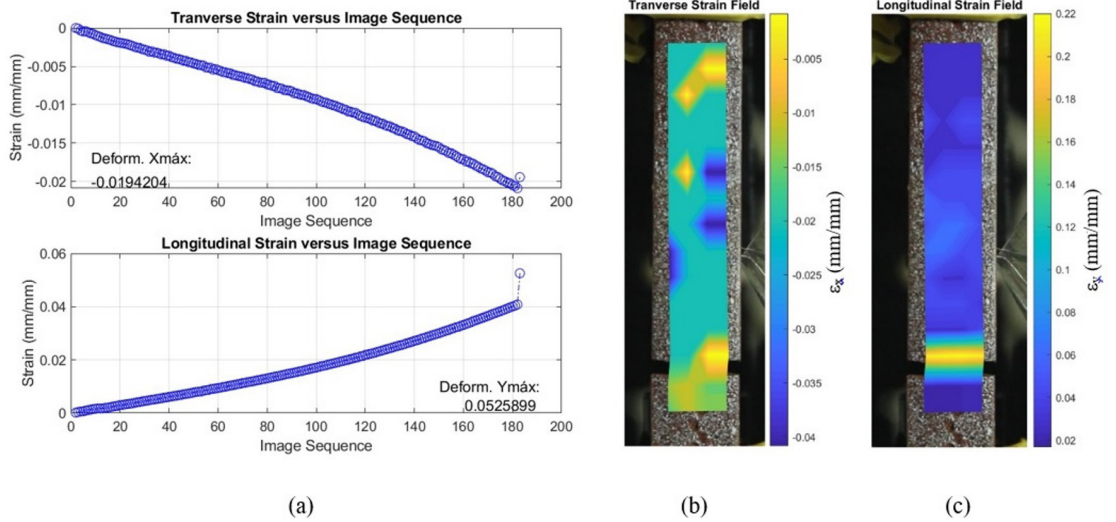


Figure 9. Deformations obtained by means of digital image correlation for sample CP02LV20 with a 30 x 5 rectangular grid. (a) Average deformations in the transverse and longitudinal directions. (b) Transverse deformation fields. (c) Longitudinal deformation fields.

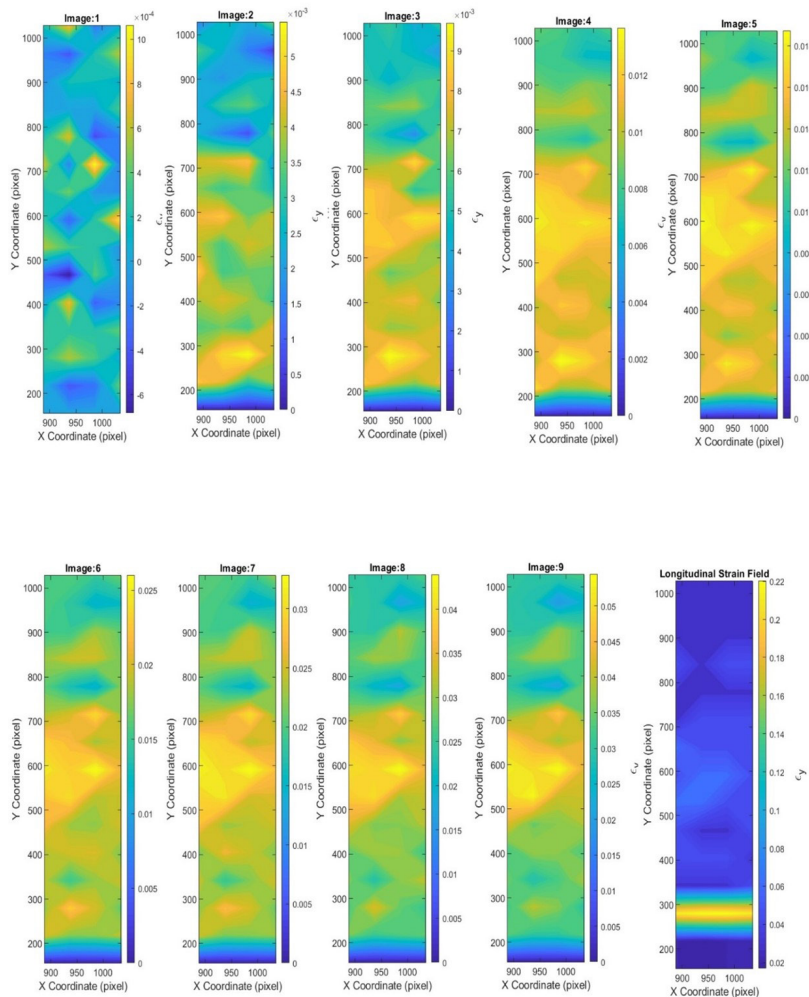
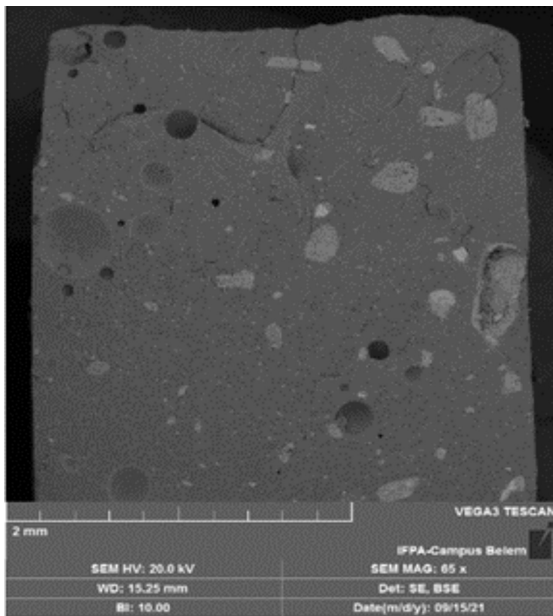


Figure 10. Partial longitudinal strain fields obtained by means of DIC for the test under traction of the specimen CP02LV20.

Table 5. Analysis of variance for composites with red mud.

Total Strain (mm/mm)						
Source	Sum of Squares	Degrees of Freedom	Mean of Squares	F (Calculated)	F Critical	P-value
Between the groups	1.20×10^{-6}	1	1.20×10^{-6}	1.86×10^{-2}	4.96	0.894
Inside the group	6.47×10^{-4}	10	6.47×10^{-5}			
Total	6.48×10^{-4}	11				
Young's Modulus (GPa)						
Source	Sum of Squares	Degrees of Freedom	Mean of Squares	F (Calculated)	F Critical	P-value
Between the groups	6.35×10^{-4}	1	6.35×10^{-4}	1.82×10^{-2}	4.96	0.678
Inside the group	3.49×10^{-2}	10	3.49×10^{-3}			
Total	3.55×10^{-2}	11				

**Figure 11.** Cross-section of matrix composite sample.

For the longitudinal strain, the $F_{\text{calculated}}$ (1.86×10^{-2}) was lower than the $F_{\text{tabulated}}$ (4.96) at the significance level $\alpha=5\%$, it can be said that there is no significant difference for the treatments. In this way, H_0 is accepted. Similar behavior was observed for the modulus of elasticity where $F_{\text{calculated}}$ (1.82×10^{-2}) was lower than $F_{\text{tabulated}}$ (4.96) at the significance level $\alpha=5\%$, it can also be said that there is no significant difference for the treatments. In this way, H_0 is accepted. As H_0 was not rejected, the Tukey test is not necessary for both treatments.

4. Summary and Conclusions

Polyester matrix composites with red mud industrial waste, were fabricated with 20wt% waste. The mechanical properties in traction were determined with the strains obtained by electrical clip-on Extensometer and by digital image correlation (DIC) applying a 30 x 5 rectangular grid over the region of interest. The strains surveyed were compared to verify the accuracy of DIC and the fields of

deformations were evaluated for the verification of the failure mechanisms. Based on the results obtained in this research work, the following conclusions can be drawn:

- The modulus of elasticity measured by extensometer and via DIC differed by an average of 2.20% and the failure strain showed average differences of 1.61%, reinforcing the efficiency of the DIC technique in obtaining the average strain on the surface of the samples.
- Statistical analysis showed no significant difference between the results obtained in the two techniques for the modulus and failure strain, at a significance level of 5%.
- The average longitudinal strains obtained via DIC during the test allowed the comparison of the stress-strain diagrams generated with those obtained via strain gauge. The mean difference between the strains compared was 0.11%, calculated for the six samples tested.
- The full-field deformation generated allowed for verifying the localized deformations occurring on the surface of the sample under test, precisely identifying the fracture region.
- The partial full-field deformation generated did not make it possible to previously identify the fracture regions due to the fragile nature of the fracture observed in particulate polymeric composites.
- Under the conditions tested, it is still necessary to evaluate the strain rate applied during the test and the need to expand the analysis to DIC-3D in order to fully identify the failure mechanisms occurring when carrying out the test.

5. Acknowledgements

The authors thank support to this investigation by the Brazilian agencies: CNPq, CAPES; UFPA, and IFPA for providing our research facilities and their support to this manuscript.

6. References

1. Hassan GM. Deformation measurement in the presence of discontinuities with digital image correlation: a review. *Opt Lasers Eng.* 2021;137:106394.

2. Mayo-Corrochano C, Sánchez-Aparicio LJ, Aira JR, Sanz-Arauz D, Moreno E, Melo JP. Assessment of the elastic properties of high-fired gypsum using the digital image correlation method. *Constr Build Mater.* 2022;317:125945.
3. Özaslan E, Yeting A, Acar B, Güler MA. Damage mode identification of open hole composite laminates based on acoustic emission and digital image correlation methods. *Compos Struct.* 2021;274:114299.
4. Castillo ER, Allen T, Henry R, Griffith M, Ingham J. Digital image correlation (DIC) for measurement of strains and displacements in coarse, low volume-fraction FRP composites used in civil infrastructure. *Compos Struct.* 2019;212:43-57.
5. Dong YL, Pan B. A review of speckle pattern fabrication and assessment for digital image correlation. *Exp Mech.* 2017;57:1161-81.
6. Zhang Y, Zhang A, Zhen Z, Lv F, Chu PK, Ji J. Red mud/polypropylene composite with mechanical and thermal properties. *J Compos Mater.* 2011;45(26):2811-6.
7. Prabu VA, Johnson RDJ, Amuthakkannan P, Manikandan V. Usage of industrial wastes as particulate composite for environment management: hardness, tensile and impact studies. *J Environ Chem Eng.* 2017;5(1):1289-301.
8. Vigneshwaran S, Uthayakumar M, Arumugaprabu V. Potential use of industrial waste-red mud in developing hybrid composites: a waste management approach. *J Clean Prod.* 2020;276:124278.
9. Vigneshwaran S, Uthayakumar M, Arumugaprabu V. Development and sustainability of industrial waste-based red mud hybrid composites. *J Clean Prod.* 2019;230:862-8.
10. Kan L, Wang F, Zhang Y, Wei Y, Wu M. An exploratory study on use red mud waste as a replacement for fly ash to prepare engineered cementitious composites. *Constr Build Mater.* 2022;342:127900.
11. Ding C, Zhang Y, Zhang N, Di X, Li Y, Zhang Y. A new insight into utilization of red mud in poly (vinyl chloride) composites via surface modification and toughening modulation to attain performance optimization. *Constr Build Mater.* 2022;333:127340.
12. Das O, Babu K, Shanmugam V, Sykam K, Tebyetekerwa M, Neisiany RE et al. Natural and industrial wastes for sustainable and renewable polymer composites. *Renew Sustain Energy Rev.* 2022;158:112054.
13. Liu L, Zhang Y, Lv F, Yang B, Meng X. Effects of red mud on rheological, crystalline and mechanical properties of red mud/PBAT composites. *Polym Compos.* 2016;37(7):2001-7.
14. Panda S, Behera D. Effect of red mud on mechanical and chemical properties of unsaturated polyester-epoxy-bambu fiber composites. *Mater Today Proc.* 2017;4(2):3325-33.
15. ASTM: American Society for Testing and Materials. ASTM D638: standard test method for tensile properties of plastics. West Conshohocken: ASTM; 2014.
16. Niu Y, Wang J, Shao S, Wang H, Lee H, Park SB. A comprehensive solution for electronic packages reliability assessment with digital image correlation (DIC) method. *Microelectron Reliab.* 2018;87:81-8.
17. Liu RX, Poon CS. Utilization of red mud derived from bauxite in self-compacting concrete. *J Clean Prod.* 2016;112:384-91.
18. Wang W, Chen W, Liu H, Han C. Recycling of waste red mud for production of ceramic floor tile with high strength and lightweight. *J Alloys Compd.* 2018;748:876-81.
19. Lima MSS, Thives LP. Evaluation of red mud as filler in Brazilian dense graded asphalt mixtures. *Constr Build Mater.* 2020;260:119894.
20. Zhang J, Li P, Liang M, Jiang H, Yao Z, Zhang X et al. Utilization of red mud as an alternative mineral filler in asphalt mastics to replace natural limestone powder. *Constr Build Mater.* 2020;237:117821.
21. Zhang J, Yao Z, Wang K, Wang F, Jiang H, Liang M et al. Sustainable utilization of bauxite residue (red mud) as a road material in pavements: a critical review. *Constr Build Mater.* 2021;270:121419.
22. Yoon K, Jung JM, Cho DW, Tsang DCW, Kwon EE, Song H. Engineered biochar composite fabricated from red mud and lipid waste and synthesis of biodiesel using the composite. *J Hazard Mater.* 2019;366:293-300.
23. Qiu L, Phule AD, Han Y, Wen S, Zhang ZX. Thermal aging, physico-mechanical, dynamic mechanical properties of chlorinated polyethylene/red mud composites. *Polym Compos.* 2020;41(11):4740-9.
24. Ma H, Sun Z, Wei J, Zhang X, Zhang L. Utilization of modified red mud waste from the Bayer process as subgrade and its performance assessment in a large-sale application. *Coatings.* 2022;12(4):471.
25. Quanjin M, Rejab MRM, Halim Q, Merzuki MNM, Darus MAH. Experimental investigation of tensile test using digital image correlation (DIC) method. *Mater Today Proc.* 2020;27:757-63.